Apportioning sources of organic matter in streambed sediments: An integrated hydrogen and carbon stable isotope approach

Richard J. Cooper[1], Nikolai Pedentchouk[1], Kevin M. Hiscock[1], Paul Disdle[1], Tobias Krueger[2], Barry G. Rawlins[3],

[1]*School of Environmental Sciences, University of East Anglia, Norwich Research Park, Norwich, NR4 7TJ, UK*

[2] *IRI THESys, Humboldt University, 10099 Berlin, Germany*

[3] *British Geological Survey, Keyworth, Nottingham, NG12 5GG, UK*

[*] Correspondence: Richard.J.Cooper@uea.ac.uk

GRAPHICAL ABSTRACT

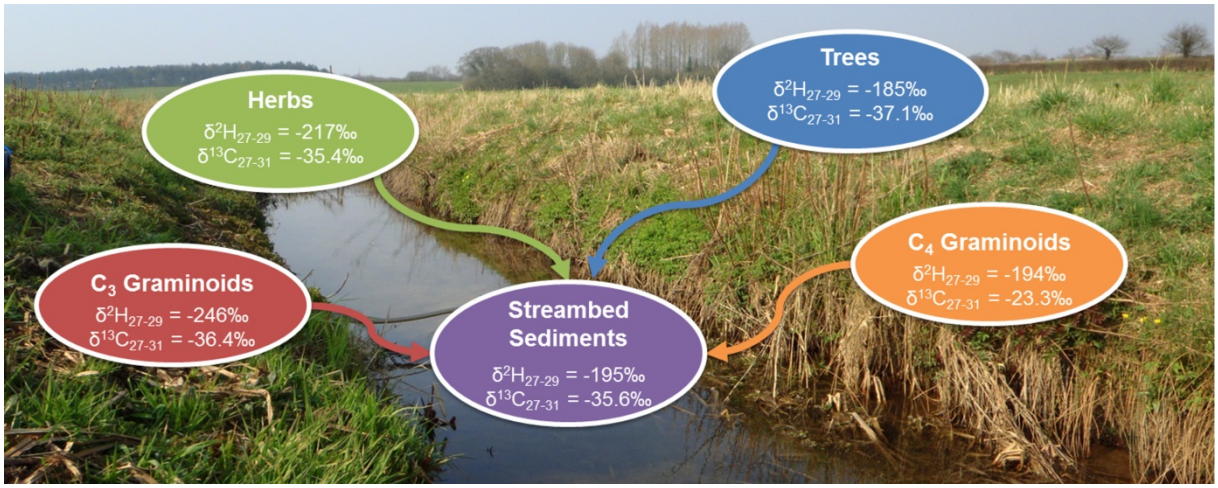

ABSTRACT

We present a novel application for quantitatively apportioning sources of organic matter in streambed sediments via a coupled δ^2H and $\delta^{13}C$ compound-specific isotope analysis (CSIA) of leaf wax *n*-alkane biomarkers using a Bayesian mixing model. Leaf wax extracts of 13 plant species were collected from across three sub-environments (aquatic, bankside and terrestrial) and four plant functional types (trees, herbaceous perennials and C_3 and C_4 graminoids) from the agricultural River Blackwater catchment, Norfolk, UK. Nine isotopic ratio and *n*-alkane chain length fingerprints were derived, which successfully differentiated 93% of individual plant specimens by plant functional type. The δ^2H values were the strongest discriminators of plants originating from different functional groups, with trees (mean values ranging from -208‰ to -164‰) and C_3 graminoids (mean values ranging from -259‰ to -221‰) providing the largest contrasts. The $\delta^{13}C$ values provided strong distinction between C_3 and C_4 plants, and successfully discriminated between natural and cultivated vegetation. *n*-Alkane chain length metrics complemented hydrogen and carbon isotope data by

discriminating between aquatic, bankside and terrestrial sub-environments. Neither δ^2H nor $\delta^{13}C$ could uniquely identify plants based on sub-environment, emphasizing a stronger plant physiological/biochemical rather than environmental control over isotopic differences. Bayesian source apportionment results for 18 streambed sediments collected between September 2013 and March 2014, revealed considerable temporal variability in organic matter sources. Median organic matter contributions ranged from 22-52% for trees, 29-50% for herbaceous perennials, 17-34% for C_3 graminoids and 3-7% for C_4 graminoids. The results presented here clearly demonstrate the effectiveness of an integrated stable isotope and molecular approach for quantitatively apportioning plant specific organic matter contributions to streambed sediments. Future research could investigate whether soils under particular vegetation types are tagged with unique δ^2H and $\delta^{13}C$ signatures that would allow these isotopes to be used as direct land-use specific soil erosion tracers.

HIGHLIGHTS

- Organic contributions from trees, herbs and C_3/C_4 graminoids are apportioned.
- δ^2H provides strong discrimination between plant functional types.
- $\delta^{13}C$ provides strong contrasts between C_3 and C_4 plants.
- δ^2H and $\delta^{13}C$ values were not influenced by sub-environment.
- *n*-Alkane chain length metrics compliment isotopic discrimination.

Keywords: Fingerprinting; *n*-alkanes; CSIA; Bayesian; mixing model; agricultural land-use

1. INTRODUCTION

Sediment fingerprinting has become a popular technique for apportioning the sources of deposited and suspended sediments across a range of aquatic environments via a mixing model approach (Mukundan *et al*., 2012; Guzmán *et al*., 2013; Walling, 2013). As the number and type of source apportionment studies have increased over recent years, there has been a shift in research focus towards re-evaluating and advancing existing fingerprinting procedures (e.g. Koiter *et al*., 2013; Cooper *et al*., 2014a; Smith and Blake, 2014; Laceby and Olley, 2014; Pulley *et al*., 2015). Because the majority of existing fingerprinting studies have focused solely on inorganic sediment provenance (e.g. Collins *et al*., 2013; Thompson *et al*., 2013; Wilkinson *et al*., 2013), the apportionment of organic matter in fluvial sediments in agricultural settings remains largely undeveloped. Understanding the origins of fluvial organic matter is important because organic material can constitute a significant percentage of the total sediment volume (e.g. Cooper *et al*., 2014b). Furthermore, elevated organic matter concentrations are associated with enhanced transport of nutrients and heightened biological oxygen demand, thus leading to the degradation of water quality (Evans *et al*., 2004; Hilton *et al*., 2006; Withers and Jarvie, 2008). Whilst an understanding of the amount of organic material transported in fluvial systems can be achieved by monitoring the fluxes of

dissolved and particulate organic carbon at the catchment outlet (Alvarez-Cobelas *et al*., 2012; Némery *et al*., 2013), such measurements are unable to yield quantitative information on the specific sources of this organic load.

Addressing this matter, compound-specific isotope analysis (CSIA) has the potential to facilitate identification of organic matter contributions to riverine sediments by exploiting differences in the stable isotopic composition amongst different plants at either the species or plant functional type level (Marshall *et al*., 2007). Of particular interest in this study are the carbon ($\delta^{13}C$) and hydrogen ($\delta^{2}H$) stable isotopic compositions of plant *n*-alkanes. Although *n*-alkanes represent only a small fraction of total organic matter, these compounds have unique biological origins which allow them to be used as plant specific biomarkers of organic matter contributions (Meyers, 1997). Compared with other plant biochemical components, such as carbohydrates, amino acids and lignin, *n*-alkanes also persist in the environment due to a high resistance to degradation (Bourbonniere and Meyers, 1996), thus making them suitable conservative fingerprints for sediment source apportionment. Variability in the carbon and hydrogen isotopic compositions of plant *n*-alkanes are driven by a complex combination of differences in plant physiology/biochemistry and a range of environmental factors, including temperature, humidity, light availability, salinity and the isotopic composition of water and CO_2 (O'Leary, 1988; Farquhar *et al.*, 1989; Sessions *et al*., 1999; Hou *et al*., 2007; Sachse *et al*., 2012). Importantly, this means the degree of isotopic fractionation is unique for each individual plant, thereby allowing distinct *n*-alkane isotopic signatures to develop which can be used to differentiate between different plant types.

A number of studies have previously been successful in using the $\delta^{13}C$ isotopic signatures of soils and sediments to identify fluvial sediment contributions derived from allochthonous and autochthonous sources (e.g. McConnachie and Petticrew, 2006; Schindler Wildhaber *et al*., 2012), or from different land use types based on the dominant vegetation cover (e.g. Fox and Papanicolaou *et al*., 2007; Gibbs, 2008; Blake *et al*., 2012; Hancock and Revill, 2013; Laceby *et al*., 2014). However, to our knowledge, the usefulness of integrating both the $\delta^{2}H$ and $\delta^{13}C$ values of individual organic compounds for quantifying organic matter source apportionment in stream sediments has never been assessed. The main objectives of this study were, therefore:

(i) to assess the effectiveness of $\delta^{2}H$ and $\delta^{13}C$ values of *n*-alkanes from higher plants at differentiating among (a) plants derived from different functional types, (b) cultivated vs. natural species, and (c) plants growing in different sub-environments;

(ii) to determine whether *n*-alkane chain length metrics can enhance discrimination between plant groups when used in combination with isotopic ratios;

92 (iii) to demonstrate an application of these isotopic ratios and chain length metrics as
93 fingerprints within a Bayesian mixing model by quantitatively apportioning plant
94 contributions to fluvial particulate organic matter.

95 We applied this novel CSIA fingerprinting technique to streambed sediments collected over a 7-
96 month period between September 2013 and March 2014 from an agricultural headwater catchment of
97 the River Wensum, Norfolk, UK.

98 ## 2. METHODS

99 ### 2.1 Study Location

100 The River Wensum is a nutrient enriched, lowland calcareous river system, which drains an area of
101 593 km^2 in Norfolk, UK. The Wensum catchment is divided into 20 sub-catchments, one of which, the
102 20 km^2 Blackwater sub-catchment, represents the area intensively monitored as part of the River
103 Wensum Demonstration Test Catchment (DTC) project (Wensum Alliance, 2014). For observational
104 purposes, the Blackwater sub-catchment is divided into six 'mini-catchments' A to F, each of which
105 has a bankside monitoring kiosk at the outlet. The 5.4 km^2 mini-catchment A provided the focus for
106 this research (Figure 1). Situated ~40 m above sea level with gentle slopes that rarely exceed 0.5^o,
107 intensively farmed arable land constitutes 92% of this headwater catchment. A 7-course crop rotation
108 is practiced with autumn and spring sown wheat and barley, sugar beet, oilseed rape and spring beans.
109 A small and variable amount of land is also lain down to maize for game bird cover. The remainder of
110 mini-catchment A is covered by 3% improved grassland, 2% semi-natural grassland, 1.5% deciduous
111 woodland, 0.5% coniferous woodland and 1% rural settlements. From May to September, emergent
112 macrophytes dominate stream primary productivity to such an extent that the river is commonly
113 obscured from view (Figure 2a). Towards the end of the growing season (mid-October) this
114 vegetation is cleared to improve catchment drainage and prevent winter flooding of the surrounding
115 arable land (Figure 2b).

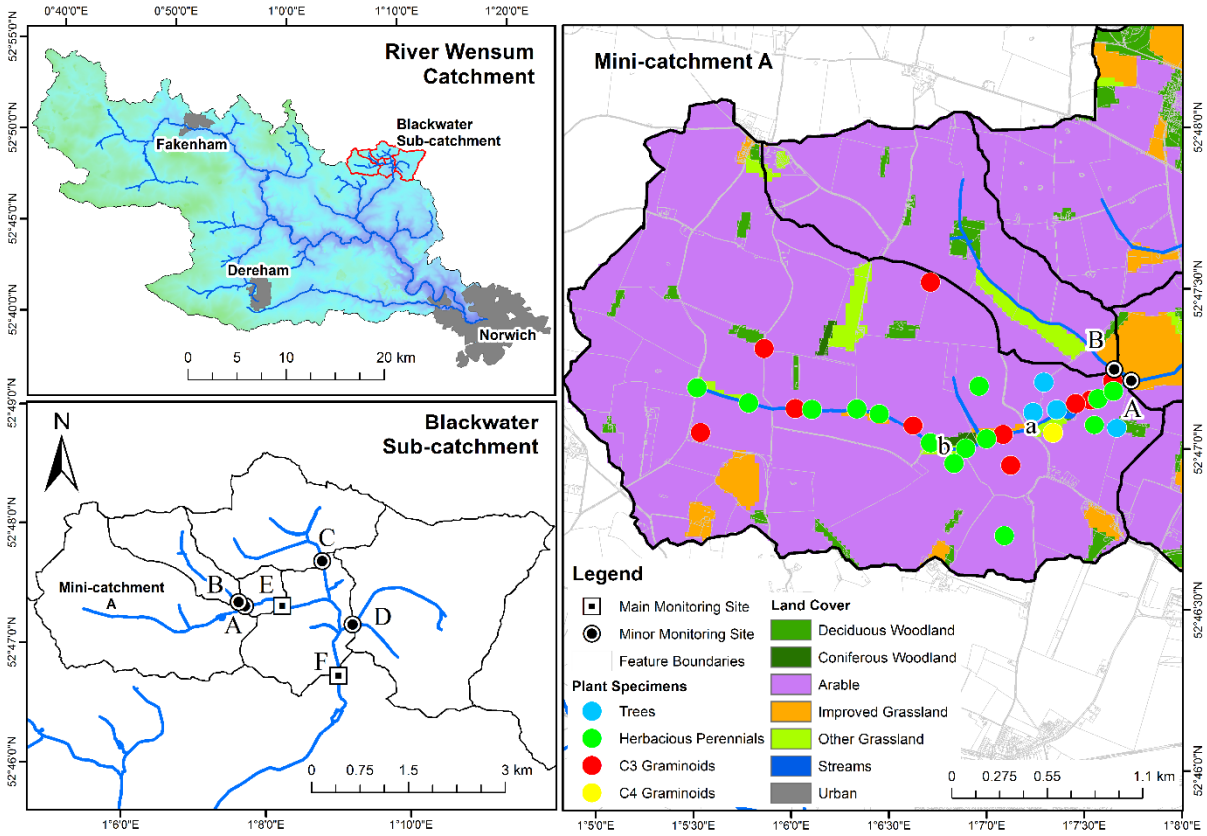

Figure 1: The Blackwater sub-catchment of the River Wensum, Norfolk, UK, showing mini-catchments A-F, surface land cover and the locations of tree, graminoid and herbaceous perennial plant collection within mini-catchment A. Lowercase a and b refer to image locations for Figure 2.

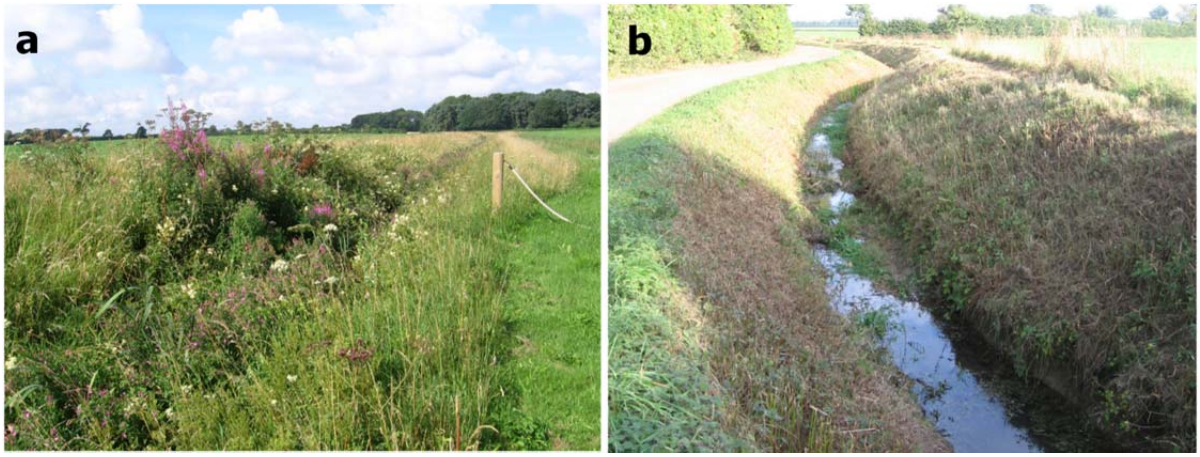

Figure 2: The River Blackwater in mini-catchment A, showing (a) the dominance of emergent macrophytes in August and (b) following vegetation clearance in October. Image locations are shown in Figure 1.

2.2 Sample Collection and Preparation

127 *2.2.1 Streambed Sediments*

128 Streambed sediments were collected at the outlet to mini-catchment A at approximately weekly
129 intervals between September 2013 and March 2014, yielding a total of 18 samples for analysis. This
130 autumn to spring period was chosen as it represents the most dynamic time with respect to catchment
131 sediment mobilization (e.g. Oeurng *et al*., 2011). Sediment volumes of 1 liter were obtained from the
132 streambed surface (approximately <50 mm depth) using a non-magnetic towel that had been
133 thoroughly washed in the stream prior to sampling. Sediments were transported back to the laboratory
134 in sealed HDPE bottles, where they were immediately oven dried at 40^{o}C for 48-72 hrs. Dried
135 sediments were lightly disaggregated using a pestle and mortar and sieved down to <63 μm to isolate
136 the biochemically important clay-silt fraction (Horowitz, 2008) in keeping with common sediment
137 fingerprinting practice (e.g. Walling *et al*., 2005). These fine sediments were stored in the dark at
138 room temperature in sealed polyethylene bags prior to analysis.

139 *2.2.2 Plant Specimens*

140 Plant leaf samples were collected across mini-catchment A during August and September 2013 for
141 organic matter source area classification. A total of 30 individual plant specimens were collected from
142 three sub-environments (aquatic, bankside and terrestrial) and four plant functional types (trees,
143 herbaceous perennials and C_3 and C_4 graminoids), and included a mixture of both cultivated and
144 natural vegetation. For aquatic plants, 12 specimens were collected, all of which were emergent
145 macrophytes owing to their dominance of stream biomass. These included the herbaceous perennials
146 *Chamerion angustifolium* (rosebay willowherb), *Aegopodium podagraria* (ground elder), *Typha*
147 *latifolia* (reed mace) and *Iris pseudacorus* (yellow flag iris), as well as three C_3 Poaceae graminoid
148 specimens. For the bankside environment, six specimens were obtained including the tree species
149 *Carpinus betulus* (hornbeam) and *Fraxinus excelsior* (ash), the herbaceous perennial *Typha latifolia*
150 (reed mace) and three C_3 Poaceae graminoids. Lastly, 12 specimens of both natural and cultivated
151 origin were obtained from the terrestrial environment, which in this study was defined as any
152 location >5 m from the stream channel. Specimens collected included the tree species *Crataegus*
153 *monogyna* (hawthorn), *Carpinus betulus* (hornbeam) and *Acer campestre* (field maple), herbaceous
154 perennials *Raphanus sativus* (oilseed radish) and *Phaseolus vulgaris* (spring beans), the C_4 graminoid
155 *Zea mays* (maize), the C_3 graminoid *Triticum* sp. (wheat) and a further three natural C_3 Poaceae
156 graminoids. For each plant specimen, ~10 g of leaves were collected to provide sufficient material for
157 replicate sample analysis. On return to the laboratory, samples were immediately frozen at -80^{o}C prior
158 to being freeze-dried for 48 hours and stored in the dark at room temperature in sealed polyethylene
159 bags.

160 2.3 Total Organic Carbon

Total organic carbon (TOC) concentrations for the 18 streambed sediments were determined by mixing 25 mg of the fine grained sediments into suspension with 1 liter of Milli-Q water (Merck Millipore, Billerica, MA, USA), which was subsequently vacuum filtered onto quartz fiber filter (QFF) papers with a particle retention rating of 99.3% at 0.45 μm. Sediment covered filters were oven dried at 105^{o}C for 2 hrs, before being finely ground and the resulting powders analyzed directly by diffuse reflectance infrared Fourier transform spectroscopy (DRIFTS) following the procedure of Cooper *et al*. (2014c) . TOC was taken to be 58% of total organic matter (Broadbent, 1953).

2.4 *n*-Alkane Extraction

Two different techniques were required to extract aliphatic *n*-alkanes from streambed sediments and plant materials. For sediments requiring a more polar solvent to extract both the free and mineral-associated organic material, samples were mixed with Ottawa sand in a 4:1 sand-sediment ratio to improve volatilization of material prior to being run through a Dionex Accelerated Solvent Extractor (ASE) 200^{TM} with HPLC grade dichloromethane solvent operated at 100^{o}C and 1500 psi. For plant specimens, alkanes were extracted by repeated sonication (3 x 10 min) of 2 g of leaf material in HPLC grade hexane. This procedure was duplicated for all 30 specimens using different leaves from the same plant to enable evaluation of isotopic variability within individual plants. Extracts from both plants and sediments were concentrated down to 1 ml under nitrogen gas in a Caliper Life Sciences TurboVap Workstation^{TM}. Final concentration down to dryness was made under nitrogen gas and the residues were re-dissolved in 1 ml hexane. The *n*-alkane extracts were purified by elution with hexane during column chromatography through a silica gel (70-230 mesh) stationary phase, and the resulting eluate was concentrated down to 1 ml under nitrogen gas in preparation for molecular and stable isotope analyses.

2.5 *n*-Alkane Ratios

The distribution and abundance of *n*-alkanes C_{13}-C_{34} were identified using an Aglient Technologies 7820A gas chromatogram fitted with a flame ionization detector (GC-FID). A temperature ramp of 20^{o}C min^{-1} between 50^{o}C and 150^{o}C, and 8^{o}C min^{-1} between 150^{o}C to 320^{o}C was used. Individual *n*-alkanes were identified by comparison of elution times against a known *n*-C_{16} to *n*-C_{30} standard (A. Schimmelmann, Indiana University, USA). Chain length distributions were summarized by the carbon preference index (CPI) and the average chain length (ACL) metrics following Zhang *et al*. (2006).

2.6 *n*-Alkane Carbon and Hydrogen Isotope Analyses

Compound-specific $\delta^{2}H$ and $\delta^{13}C$ values were determined using a Thermo Scientific™ Delta V™ Advantage isotope ratio mass spectrometer (IRMS) coupled with a GC-Isolink gas chromatograph. The GC oven temperature ramp was the same as that used for the GC-FID and reactor temperatures were set to 1000^{o}C for carbon and 1400^{o}C for hydrogen modes, respectively. All samples were run in

duplicate and an *n*-alkane (C_{16} to *n*-C_{30}) standard was run at the beginning and end of every sequence. $^{13}C/^{12}C$ isotopic composition was expressed relative to the Vienna Pee-Dee belemnite (VPDB) standard and $^{2}H/^{1}H$ isotopic composition relative to Vienna Standard Mean Ocean Water (VSMOW). Only compounds ubiquitous to all sediment samples and plant specimens were used as fingerprints for source apportionment. For $\delta^{13}C$, this meant the high-molecular weight *n*-alkanes C_{27}, C_{29}, and C_{31}, whilst C_{27} and C_{29} where selected for $\delta^{2}H$. Poor reproducibility of C_{31} for $\delta^{2}H$ meant it was excluded from the analysis. Abundance weighted C_{27}-C_{31} values for $\delta^{13}C$ and C_{27}-C_{29} values for $\delta^{2}H$ were included as fingerprints to account for within plant variation in chain length abundance, and were calculated as follows:

$$C_{27-29(31)}(‰) = \frac{\sum_{m=1}^{M}(\delta_m \times \alpha_m)}{\sum_{m=1}^{M}\alpha_m}$$

where δ is the isotopic value in ‰, α is the abundance in pico-volts (pV), *M* is the number of *n*-alkanes (three for $\delta^{13}C$, two for $\delta^{2}H$) and *m* is the alkane index. Mean absolute errors between replicate samples (precision) were 2‰ for $\delta^{2}H_{27}$, 1‰ for $\delta^{2}H_{29}$ and 0.1‰ for $\delta^{13}C_{27}$, $\delta^{13}C_{29}$ and $\delta^{13}C_{31}$.

2.7 Statistical Source Discrimination and Bayesian Apportionment

The Kruskal-Wallis one-way analysis of variance and stepwise linear discriminant analysis based on the minimization of the Wilk's Lambda criterion were employed to quantitatively determine the proportion of source area samples that could be correctly classified by selected isotopic values and *n*-alkane chain length metric fingerprints (Collins *et al.*, 2012). Principal component analysis plots were also generated to visualize the mixing space geometry. Due to differences in plant physiology/biochemistry, the abundance of *n*-alkanes produced per unit of organic matter has been shown to vary between both species and different chain lengths within the same plant (Diefendorf *et al.*, 2011; Bush and McInerney, 2013). Consequently, isotopic ratios and chain length metrics were weighted by *n*-alkane abundances when grouping fingerprints by source prior to running the Bayesian mixing model. This was calculated by replicating fingerprint values for each plant specimen *n* times, as follows:

$$J^{K} = \sum_{i=1}^{I} J_i \times (n = \alpha_i)$$

where J^K is the source abundance weighted fingerprint value; *J* is the unweighted fingerprint value; *n* is the number of replicate fingerprint values generated and is equal to α, the relative *n*-alkane abundance (pV); *I* is the number of individual plants in each source; and *i* is the individual plant index. Mean values and covariance matrices for these source abundance weighted fingerprints were then passed onto the empirical Bayesian mixing model to quantitatively apportion *n*-alkane sources. The model was run in the open source software JAGS 3.3.0 (Just Another Gibbs Sampler; Plummer, 2003) within the R environment (R Development Core Team, 2013). Full structural details of the model

employed can be found in the supplementary information (see also Cooper *et al*., 2014a). In summary, samples were drawn from the joint posterior probability density function of the variables of interest:

$$p\left(S, \Phi, \Sigma^{resZ}, \mu^{\Phi}, \sigma^{2\Phi} | Y\right) \propto p(Y|S, \Phi, \Sigma^{resZ}) \cdot p(S) \cdot p\left(\Phi|\mu^{\Phi}, \sigma^{2\Phi}\right) \cdot p(\Sigma^{resZ}) \cdot p\left(\mu^{\Phi}\right) \cdot p\left(\sigma^{2\Phi}\right)$$

where Y, the concentration of each fingerprint in streambed sediment organic matter, is a function of the concentration of that fingerprint in each plant source group, S, multiplied by the proportional organic matter contribution from each source, P=ILR^{-1}(Φ). Φ are isometric log-ratio (ILR) transformed proportions (P); Σ^{resZ} is the combined instrument and residual error; Σ are covariance matrices; σ^2 are variances; and μ are means. A Markov Chain Monte Carlo (MCMC) sampling procedure of the full parameter distributions was run using three parallel chains of 250,000 iterations each with a 100,000 sample burn-in and a 225 sample jump length to ensure model convergence and minimize autocorrelation between sample runs. A further correction was required to convert the mixing model *n*-alkane source apportionment results into contributions of organic matter and was applied as follows:

$$P_{OM} = \frac{\frac{P_k}{\alpha_k}}{\sum_{k=1}^{K}\left(\frac{P_k}{\alpha_k}\right)}$$

where P_{OM} is the corrected contribution of organic matter from each source; P is the mixing model estimated proportion of *n*-alkanes; α is the mean relative *n*-alkane abundance for each source; K is the number of sources; and k is the source index.

3. RESULTS AND DISCUSSION

The individual and collective effectiveness of δ^2H, δ^{13}C and *n*-alkane chain length metrics as fingerprints for differentiating between plants derived from different functional types, between cultivated and natural species and between plants derived from different sub-environments were assessed in turn. The strongest discriminators were then used to quantitatively apportion, with uncertainty, the sources of organic matter in streambed sediments via the comprehensive Bayesian mixing model.

3.1 Isotopes for Discriminating Plant Functional Types

3.1.1 Hydrogen

CSIA of the 13 plant species collected from across mini-catchment A revealed that δ^2H provided strong discrimination between some of the plant functional groups (Figure 3a; Table 1). Tree species (*Fraxinus excelsior*, *Carpinus betulus*, *Crataegus monogyna* and *Acer campestre*) exhibited the most ^{2}H-enriched isotopic composition, with $\delta^2H_{27\text{-}29}$ values ranging from -208‰ to -164‰, with an *n*-

alkane abundance weighted mean of -185‰. This contrasted strongly with the C_3 graminoids which had the lowest $\delta^2H_{27\text{-}29}$ values, ranging from -259‰ to -221‰ with an abundance weighted mean of -246‰. The majority of species representing the herbaceous perennials group (-223‰ to -172‰), which included both natural (*Typha latifolia*, *Aegopodium podagraria*, *Chamerion angustifolium* and *Iris pseudacorus*) and cultivated (*Phaseolus vulgaris* and *Raphanus sativus*) species, overlapped with trees, though some had $\delta^2H_{27\text{-}29}$ values closer to C_3 graminoids. The herbaceous perennial group had an abundance weighted mean of -216‰. The C_4 graminoid *Zea mays* (-195‰), the only C_4 species in this study, was ^{2}H-enriched by ~50‰ relative to the C_3 graminoids, but overlapped with trees and herbaceous perennials. Overall, there existed a sizeable 94‰ range in $\delta^2H_{27\text{-}29}$ values across all 13 plant species with a clear distinction between C_3 graminoids and the other plant functional groups, thus confirming the suitability of δ^2H as an effective discriminator and fingerprint of different plant types.

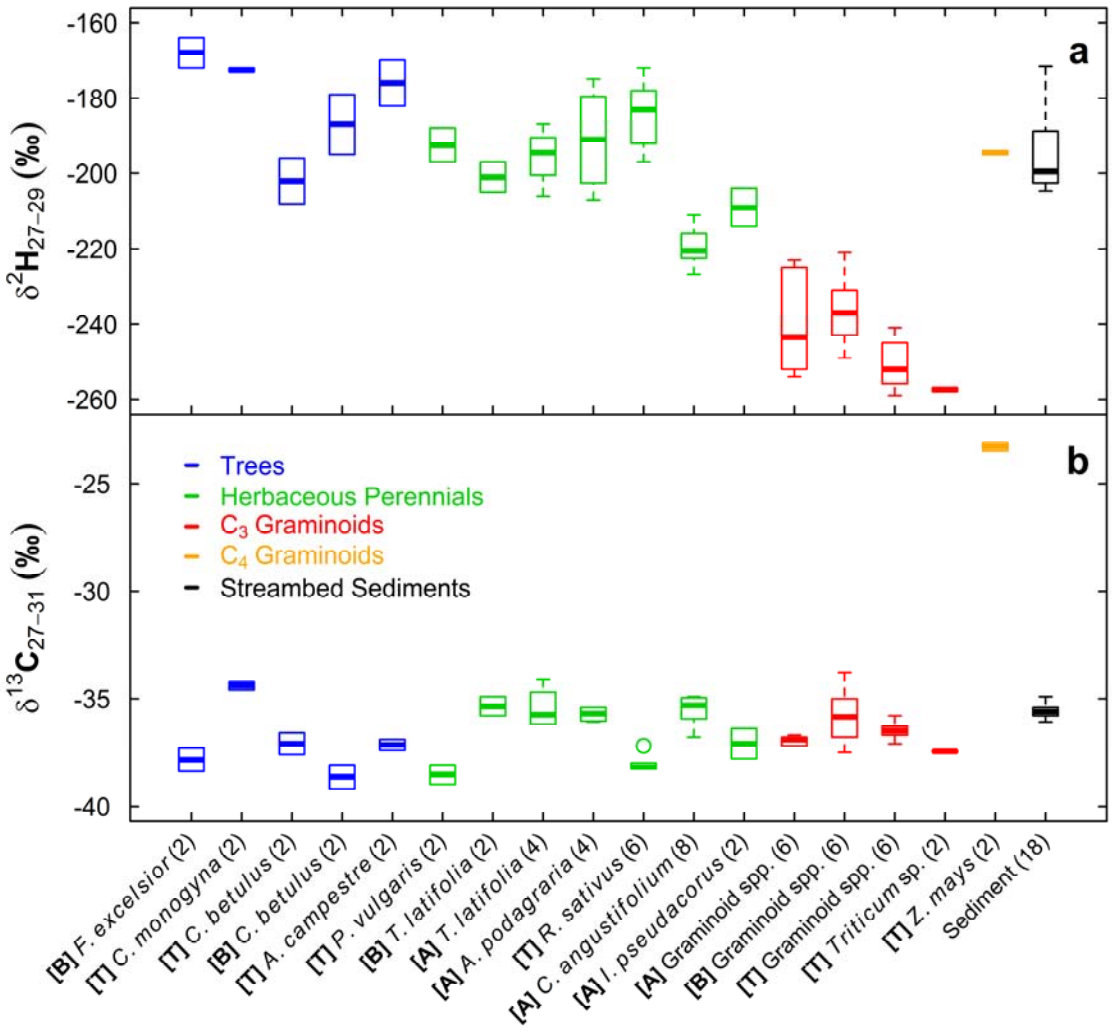

Figure 3: Distribution of δ^2H and $\delta^{13}C$ values (‰) for streambed sediments and individual plant species arranged by plant functional type. [A], [B] and [T] refer to aquatic, bankside and terrestrial sub-environments, respectively. Parentheses refer to the number of specimens for each species/sediment.

3.1.2 Carbon

The dominant interspecies distinction in $\delta^{13}C_{27\text{-}31}$ values was the ~12‰ difference between the C_4 graminoid *Zea mays* and the C_3 species (Figure 3b). Aside from this C_3 versus C_4 contrast, the range of $\delta^{13}C_{27\text{-}31}$ values for trees (-39.2‰ to -34.2‰), C_3 graminoids (-37.5‰ to -33.8‰) and herbaceous perennials (-39.0‰ to -34.1‰) had substantial overlaps which prevented discrimination based solely on $\delta^{13}C$ values. This contrasts with previous studies that, for example, identified differences in the $\delta^{13}C$ values between angiosperm and conifer species (e.g. Pedentchouk *et al*., 2008). However, there remained relatively large intra-group variability that would allow individual species identification based on $\delta^{13}C_{27\text{-}31}$ values. For example, for herbaceous perennials where *P. vulgaris* (-38.6‰) is $\delta^{13}C$-depleted relative to the other herbaceous species (-38.3‰ to -34.1‰). The $\delta^{13}C_{27\text{-}31}$ values of the streambed sediments (-36.1‰ to -34.9‰) places them firmly within the isotopic range of the C_3 plant community, indicating limited input from C_4 plants. Because such C_3 versus C_4 discrimination cannot be obtained solely from δ^2H values, the results presented here clearly support a combined $\delta^2H/\delta^{13}C$ isotopic approach for apportioning sources of organic matter, particularly in catchments with a greater abundance of C_4 vegetation.

Table 1: Summary abundance weighted *n*-alkane chain length statistics and isotopic compositions for streambed sediments and plant species grouped by plant functional type. ACL is the average chain length; CPI the carbon preference index; C_{max} the most abundant *n*-alkane. Full results for individual plant specimens are presented in supplementary Table S1.

Source/ Target	Stat.	ACL	CPI	C_{max}	$\delta^{13}C_{27}$ (‰)	$\delta^{13}C_{29}$ (‰)	$\delta^{13}C_{31}$ (‰)	$\delta^{13}C_{27\text{-}31}$ (‰)	δ^2H_{27} (‰)	δ^2H_{29} (‰)	$\delta^2H_{27\text{-}29}$ (‰)
Sediments (*n*=18)	Mean	28.9	6.5	29	-34.7	-35.7	-36.0	-35.6	-178	-203	-195
	St. dev.	0.1	1.1	0	0.5	0.3	0.3	0.3	9	10	9
Trees (*n*=10)	Mean	29.8	12.3	31	-35.3	-38.1	-37.3	-37.1	-163	-193	-185
	St. dev.	0.5	5.6	1	1.0	1.4	1.8	1.7	12	13	14
Herbaceous Perennials (*n*=28)	Mean	29.1	12.7	29	-34.7	-35.5	-35.8	-35.4	-195	-225	-217
	St. dev.	0.5	3.5	1	0.8	0.9	0.9	0.9	11	9	10
C3 Graminoids (*n*=20)	Mean	29.3	22.7	29	-35.7	-36.5	-36.5	-36.4	-223	-254	-246
	St. dev.	0.8	8.9	1	1.4	1.2	1.2	1.1	17	13	13
C4 Graminoids (*n*=2)	Mean	30.4	13.4	31	-23.6	-23.7	-22.9	-23.3	-164	-200	-194
	St. dev.	0.1	0.1	0	0.3	0.3	0.1	0.2	1	1	1

3.2 Isotopes for Discriminating Natural vs. Cultivated Species

Our data showed that $\delta^{13}C_{27\text{-}31}$ values are successful at discriminating between natural vegetation and cultivated crop species (Figure 4a). The range of $\delta^{13}C_{27\text{-}31}$ values for the three C_3 cultivated crop species (-39.0‰ to -37.2‰; *Raphanus sativus*, *Phaseolus vulgaris*, *Triticum* sp.) was lower than that recorded for the 11 natural plant species (-39.2‰ to -33.8‰) and for the C_4 cultivated *Zea mays* (-23.3‰). No obvious environmental mechanism could explain the ^{13}C-depleted isotopic compositions of cultivated C_3 crops relative to natural vegetation, suggesting this distinction was driven primarily by physiological/biochemical differences. These findings support the conclusions of other sediment fingerprinting studies that compound-specific $\delta^{13}C$ values can indeed be useful indicators of crop specific contributions to fluvial organic matter (Gibbs, 2008; Blake *et al.*, 2012).

In contrast, $\delta^{2}H_{27\text{-}29}$ values exhibited no cultivated versus natural isotopic discrimination, with all three groups exhibiting substantial range overlaps (Figure 4a). The isotopic compositions of the 18 streambed sediments placed them firmly within the natural vegetation source range, indicating natural plant communities supplied the majority of the *n*-alkanes present within these sediments. With such cultivated versus natural vegetation discrimination absent from the $\delta^{2}H$ data, these results lend further support to adopting a dual isotopic approach for organic matter source apportionment.

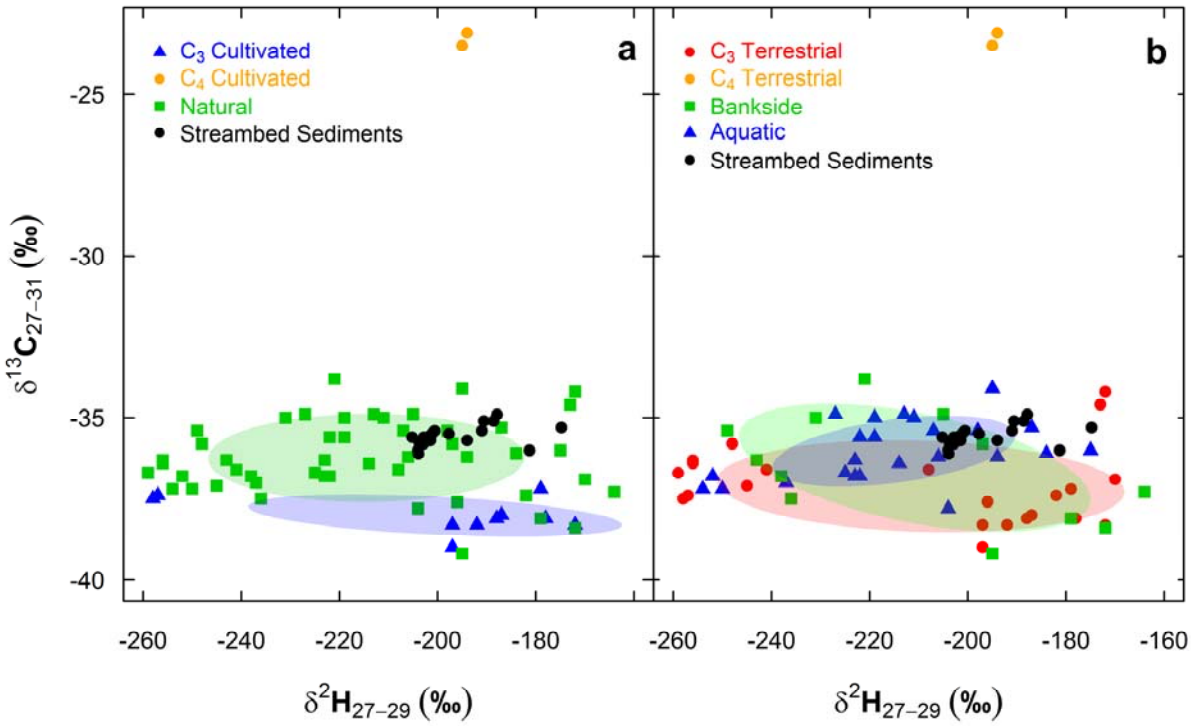

Figure 4: *n*-Alkane $\delta^{2}H_{27\text{-}29}$ and $\delta^{13}C_{27\text{-}31}$ isotopic mixing space plots for streambed sediments and individual plant specimens grouped by (a) sub-environment and (b) cultivated vs. natural vegetation. Shaded ellipsoids cover 50% of group range.

316

317 3.3 Isotopes for Discriminating Sub-Environment

318 The sub-environment in which plants were growing (i.e. terrestrial, bankside or aquatic) exerted no
319 obvious control over δ^2H or $\delta^{13}C$ values, as revealed by significant overlap between groups in isotopic
320 mixing space (Figure 4b). Mean isotopic values were marginally more enriched in C_3 terrestrial plants
321 (δ^2H = -208‰ $\pm$ 33‰; $\delta^{13}C$ = -35.9‰ $\pm$ 4.1‰) compared with aquatic (δ^2H = -215‰ $\pm$ 21‰; $\delta^{13}C$ = -
322 36.0‰ $\pm$ 0.9‰) and bankside (δ^2H = -211‰ $\pm$ 29‰; $\delta^{13}C$ = -36.5‰ $\pm$ 1.6‰) growing species,
323 however the range of values observed for all sub-environment groups was substantial. The isotopic
324 composition of the streambed sediments placed them largely within the aquatic plant source group,
325 although little can be inferred from this due to the poor sub-environment source discrimination.

326 The absence of sub-environment discrimination implies that isotopic variability among the studied
327 plants was principally driven by plant physiological and/or biochemical differences rather than the
328 growing environment. Theoretically, one might have expected lower δ^2H values in aquatic plants
329 compared to terrestrial species, because higher levels of humidity and water availability in aquatic
330 environments reduce stomatal conductance and thus lower discrimination against ^2H during
331 transpiration (Doucett *et al*., 2007; Sachse *et al*., 2012). Additionally, one might reasonably expect the
332 δ^2H values of the stream water absorbed by aquatic plants to differ from the isotopic composition of
333 the soil water used by terrestrial species, with the former being supplied by groundwater and the latter
334 by more recent precipitation. However, no evidence was observed for these mechanisms with the
335 species collected here. This can probably be explained by the shallow nature of this headwater stream
336 (mean stage = 0.25 m), where emergent macrophytes growing >1.5 m tall dominate aquatic primary
337 productivity. In contrast to submerged macrophytes, emergent species will be exposed to similar
338 environmental stressors as their terrestrial or bankside equivalents, thus weakening any sub-
339 environment driven differences. As a consequence, we cannot rule out δ^2H and $\delta^{13}C$ as potential
340 discriminators between aquatic and terrestrial organic matter sources, but merely highlight that
341 differences in growing environment, particularly in headwater streams, may not impart as large an
342 isotopic fractionation signal as physiological differences linked to plant functional type. Because of
343 these findings, plant functional type rather than sub-environment was pursued as the main source
344 group classification for apportionment

345 3.4 Alkanes for Discriminating Plant Types and Sub-Environments

346 Figure 5 presents the *n*-alkane mixing space plots of ACL and CPI for plant species grouped by (a)
347 plant functional type and (b) sub-environment. Despite considerable scatter between individuals of the
348 same group, it is apparent that tree species generally had longer ACLs (mean = 29.8 $\pm$ 0.5; Table 1)
349 than the majority of herbaceous perennials (mean = 29.1 $\pm$ 0.5), whilst the same was true for

terrestrial plants (mean = 29.6 ± 0.7) compared to aquatics (mean = 28.4 ± 0.8). For C_3 graminoids, a distinct separation existed with terrestrial graminoids having higher ACL and CPI values, whilst lower ACL and CPI values were recorded for the aquatic graminoids. Previous studies have suggested that higher *n*-alkane ACLs in paleosedimentary records can indicate greater graminoid (*n*-C_{31}) input, whilst shifts towards lower ACLs can signify more tree (*n*-C_{29}) derived organic material (Jeng, 2006; Zhang *et al*., 2006). However, the results presented here and elsewhere (e.g. Bush and McInerney, 2013) reveal that this relationship does not hold true for all species, with some tree species having higher ACLs than graminoids growing in the same environment.

Despite significant overlaps in the range of ACL and CPI values, there was stronger evidence for a sub-environmental control on these metrics than observed for either $\delta^{13}C_{27\text{-}31}$ or $\delta^{2}H_{27\text{-}29}$, although plant functional type still provided better discrimination. The mean terrestrial plant ACL (29.6 ± 0.7) and CPI (18.8 ± 10.0) were higher than that observed for aquatic ACL (28.4 ± 0.8) and CPI (12.2 ± 4.8), with mean bankside ACL (29.1 ± 0.9) and CPI (14.3 ± 6.5) located between these two sub-environments in mixing space. Whilst these *n*-alkane chain length metrics could not be used on their own to uniquely identify source groups, they do reveal potential to improve source area identification when used in combination with isotopic ratios by offering improved sub-environment discrimination.

The range of ACL values for the 18 streambed sediments (28.6 to 29.1) indicates higher plants were the dominant sources of *n*-alkanes in this river system (Jeng, 2006). In contrast, sediment CPI values ranged from 4.7 to 8.6, putting them at the lower end of the range observed across all source groups. Lower CPI values can be a sign of increased algal or microbial organic contributions (Jeng *et al*., 2006; Zech *et al*., 2011). However, a chromatogram of mean *n*-alkane chain length distributions for all 18 streambed samples (Figure 6) revealed sediments to be dominated by longer-chained *n*-alkanes with a strong odd-over-even predominance. Such distributions, coupled with terrigenous-to-aquatic ratios (TAR_{HC}) ranging from 15.5 to 64.5, are indicative of higher terrestrial plant origins (Bourbonniere and Meyers, 1996; McDuffee *et al*., 2004), thus allowing algae and bacteria to be excluded as major organic matter sources during this autumn-to-spring period. Low CPI values can also indicate contributions from ancient organic matter weathered out of the soil profile (Pancost and Boot, 2004). Depending on its age, this ancient material may reflect relic plant communities that bear little resemblance to the modern intensive arable system and therefore would not have been represented by the plants specimens collected here to classify source groups

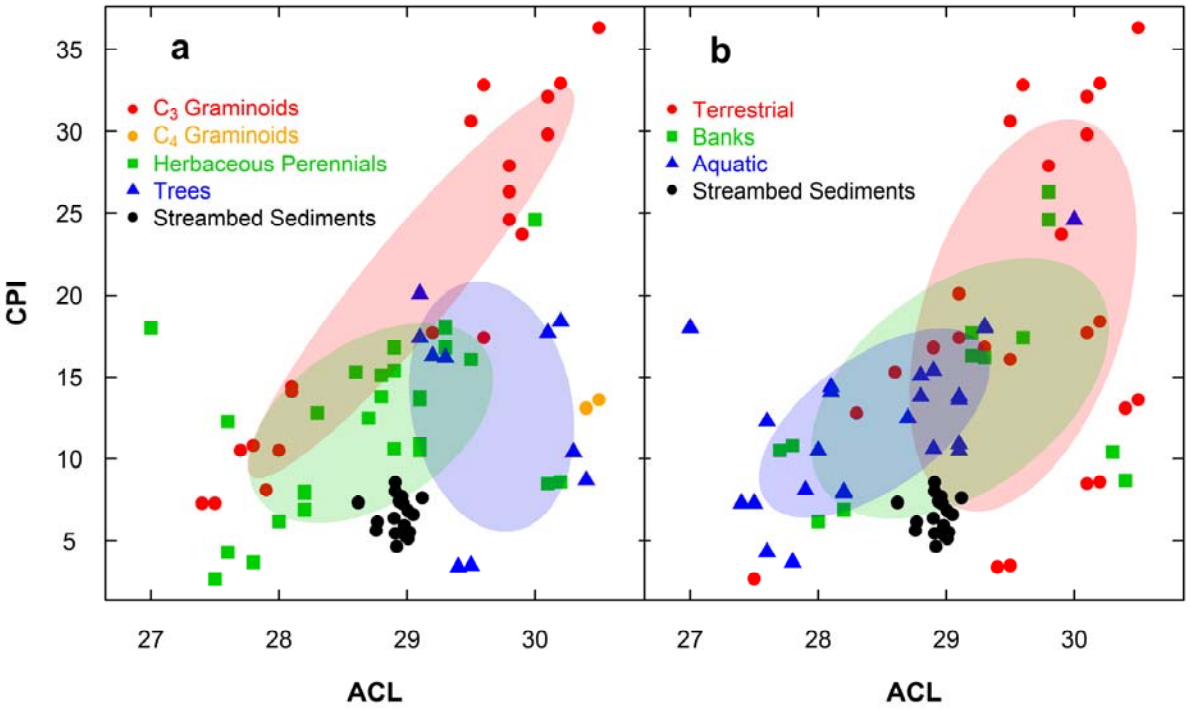

Figure 5: Average chain length (ACL) and carbon preference index (CPI) mixing space plots for streambed sediments and individual plant specimens grouped by (a) plant functional type and (b) sub-environment. Shaded ellipsoids cover 50% of group range.

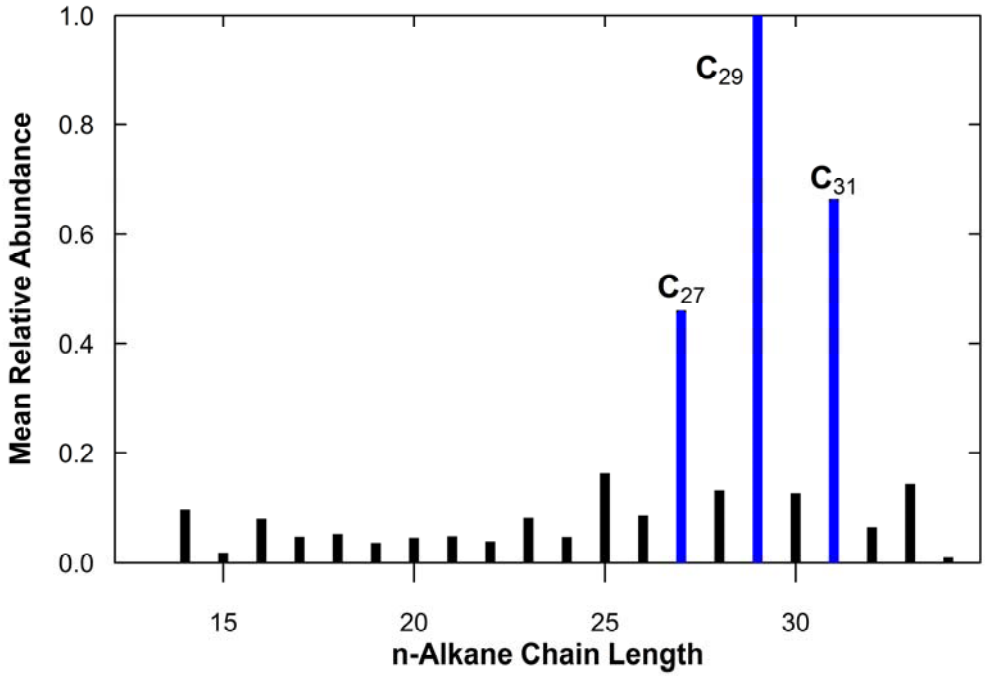

Figure 6: Chromatogram of the mean *n*-alkane chain length distribution for the 18 streambed sediment samples collected between September 2013 and March 2014, expressed relative to C_{29}. High-molecular weight *n*-alkanes ubiquitous to all samples and selected as isotopic fingerprints are highlighted in blue.

3.5 Statistical Discrimination of Isotopic and Alkane Fingerprints

Principal component analysis revealed that 95.1% of the variability between the plant species could be explained by the first three components when combining all nine of the measured isotopic and *n*-alkane chain length metric fingerprints (ACL, CPI, $\delta^{13}C_{27}$, $\delta^{13}C_{29}$, $\delta^{13}C_{31}$, $\delta^{13}C_{27\text{-}31}$, $\delta^{2}H_{27}$, $\delta^{2}H_{29}$ and $\delta^{2}H_{27\text{-}29}$). PC1, which explained 43.69% of data variance, weighed most heavily upon the four $\delta^{13}C$ fingerprints, with the more positive $\delta^{13}C$ values of C_4 graminoids providing the greatest distinction (Figure 7). The second principal component (33.92% of data variance) highlighted hydrogen isotope composition as a powerful discriminator between the ^{2}H-depleted C_3 graminoids and the comparatively ^{2}H-enriched herbaceous perennials and trees. In the third component (17.51% of variance), ACL was the dominant discriminator, with higher ACL values for trees (mean = 29.7) helping to distinguish this group from the herbaceous perennials (mean = 28.8) and C_3 graminoids (mean = 29.0). CPI was also an important distinguishing metric, with values increasing from herbaceous perennials (mean = 12.3), to trees (mean = 13.2) and finally C_3 graminoids (mean = 20.8).

The Kruskal-Wallis one-way analysis of variance revealed that eight out of the nine fingerprints could successfully differentiate between plant functional types at the 0.05 significance level (Table 2). Whilst previous studies have used failure to pass this test as a fingerprint rejection criterion in traditional frequentist source apportionment studies (e.g. Collins *et al*., 2012; Evrard *et al*., 2013), other research has demonstrated that maximizing the number of fingerprints used in Bayesian mixing models can help to significantly improve differentiation and reduce model uncertainties (Parnell *et al*., 2010). All nine fingerprints were therefore passed onto the Bayesian mixing model. In combination, the minimization of Wilks-Lambda procedure revealed 93.1% of plant specimens could be correctly classified by plant functional type from these nine fingerprints, with $\delta^{13}C_{31}$ and $\delta^{2}H_{27\text{-}29}$ being the most important discriminants.

Table 2: Kruskal-Wallis one-way analysis of variance and minimization of Wilks-Lambda fingerprint discrimination statistics.

	Kruskal-Wallis		**Minimization of Wilks-Lambda**				
Fingerprint Property	***H*-value**	***p*-value**	**Selection step**	**Wilks-Lambda**	***F*-value**	**Cumulative *p*-value**	**Cumulative % of sources correctly classified**
$\delta^{13}C_{31}$	10.14	0.017	1	0.167	89.9	<0.001	51.7
$\delta^{2}H_{27\text{-}29}$	42.32	<0.000	2	0.043	68.0	<0.001	82.8
ACL	13.48	0.004	3	0.034	42.3	<0.001	84.5
$\delta^{13}C_{27}$	7.39	0.060	4	0.028	32.3	<0.001	89.7
$\delta^{2}H_{29}$	40.08	<0.000	5	0.024	26.4	<0.001	93.1
$\delta^{13}C_{27\text{-}31}$	8.24	0.041	6	0.021	22.6	<0.001	93.1
$\delta^{2}H_{27}$	41.95	<0.000	7	0.019	19.8	<0.001	93.1
$\delta^{13}C_{29}$	9.18	0.027	8	0.017	17.6	<0.001	93.1
CPI	8.34	0.039	9	0.016	15.5	<0.001	93.1

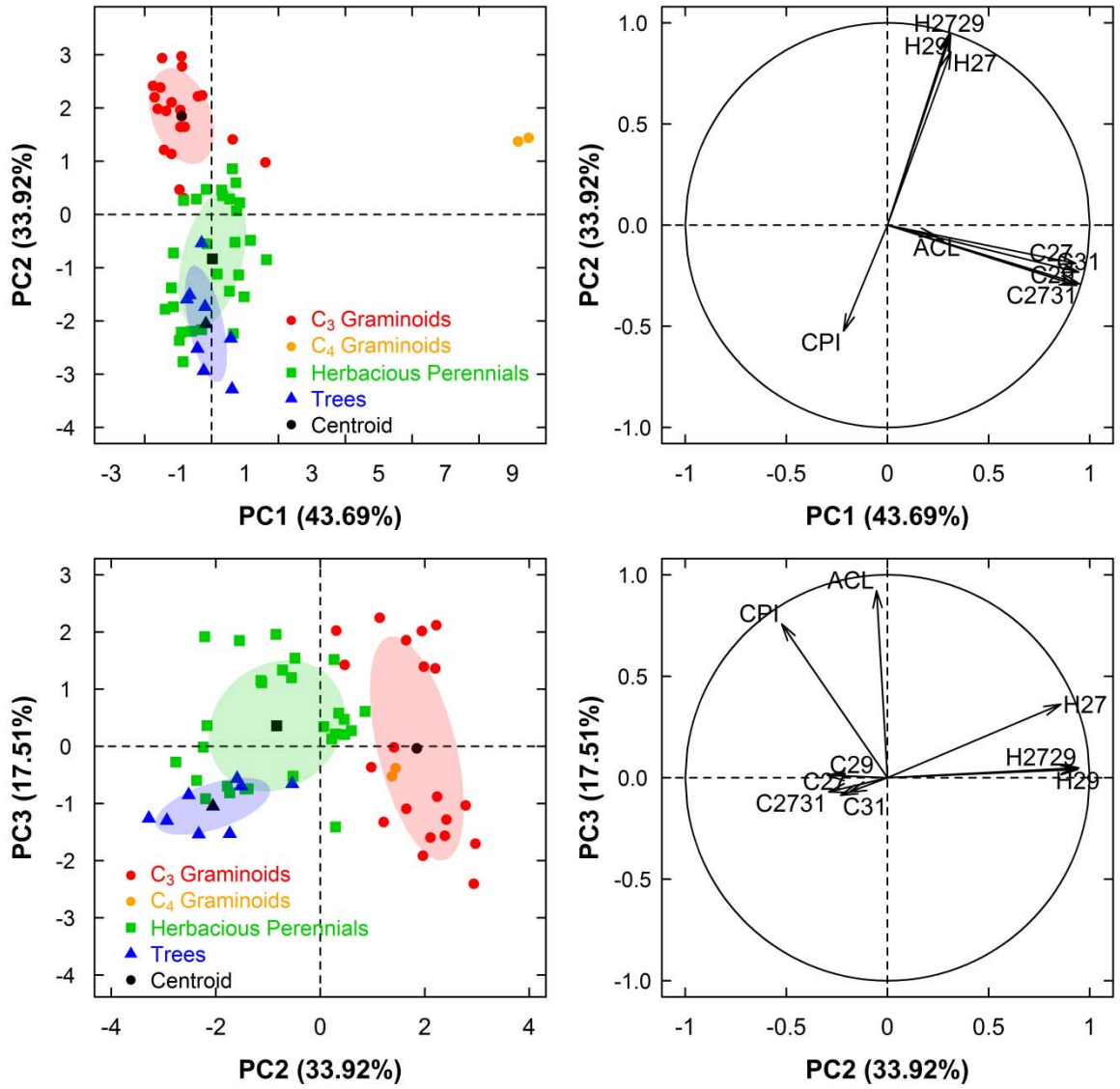

Figure 7: Principal component analysis of plant functional type sources (left) and fingerprint loadings (right) for the first three components. Shaded ellipsoids encompass 50% of the data range.

3.6 Application of the Bayesian Source Apportionment Mixing Model

The 7-month time-series of organic matter source contributions to fine (<63 µm) streambed sediments in the River Blackwater catchment, as estimated by the nine fingerprint Bayesian mixing model, are presented in Figure 8. Over the entire September 2013 to March 2014 period, TOC concentrations varied between 3-7% of total sediment volume, which is considerably lower than the 10-13% recorded for suspended particulate matter (SPM) collected at the same time from the same site (data not shown). Although *n*-alkanes represent only a small fraction of this total organic material, their conservative nature means we can work on the assumption that the sources of *n*-alkane biomarkers are representative of the sources of the entire organic matter content of the streambed sediments. In this regard, herbaceous perennials were estimated to account for a mean 39% (13-65% at the 95% credible

interval) of sediment organic matter, with a further 33% (12-54%) from trees, 26% (7-46%) from C_3 graminoids and just 4% (0-16%) from C_4 graminoids. The high contribution from herbaceous plants is consistent with the dominance of emergent herbaceous macrophytes in the stream channel during the summer months (Figure 2a). Similarly, whilst only 1.5% of the catchment is deciduous woodland, significant tree contribution was not surprising given the proximity of deciduous trees to the stream. There is also an extensive network of *Crataegus monogyna* and *Acer campestre* hedgerows across the catchment, which most likely contributed significant quantities of tree derived organic material following leaf fall during the autumn and winter period.

In spite of the relatively low precision of the proportional contributions, which arises as a consequence of the comprehensive Bayesian treatment of all perceived uncertainties (Cooper *et al*., 2014a), considerable temporal variability in apportionment estimates was still apparent. Median contributions from trees ranged from 22-52% (3-70% at the 95% credible interval), herbaceous perennials from 29-50% (2-67%) and C_3 graminoids from 17-34% (4-58%). By contrast, median C_4 graminoid contributions were consistently low across all 7 months at 3-7% (0-22%). As expected from the principal component analysis, variability in sediment $\delta^2H_{27\text{-}29}$ values appeared to exert the dominant control over estimated source contributions. Increases in $\delta^2H_{27\text{-}29}$ values were generally associated with increases in tree contribution and declines in C_3 graminoid supply, reflecting the more positive δ^2H values of tree derived organic material (Figure 3). Declines in sediment ACL, most notably that occurring in late-February 2014, were associated with increased C_3 graminoid input, whilst the decline in ACL and CPI in November 2013 was associated with a reduced herbaceous perennial contribution. None of the source contributions were found to correlate with either stage or weekly precipitation totals. However, TOC concentrations where significantly (p<0.05) positively correlated with herbaceous perennial (R^2 = 0.275) and C_3 graminoid (R^2 = 0.119) contributions, whilst being negatively correlated with contributions from trees (R^2 = -0.387).

Despite this variability in source apportionment estimates at the weekly timescale (Figure 8), there was no strong seasonality to estimated contributions, in contrast to what one might intuitively expect considering the strong seasonal nature of plant growth. Whilst tree contribution does increase by 17% during early October, which may relate to autumn leaf fall, this cannot directly explain the peak in tree contribution at 52% during mid-February 2014. Similarly, whilst herbaceous perennial contribution is marginally higher (mean = 43%) during the September to November die-back of emergent macrophytes than during the December to March period (mean = 38%), the trend is not significant within the 95% uncertainty intervals of the model. Previous research has shown the δ^2H values of individual plant species can vary seasonally in response to environmental stressors (e.g. temperature) by up to 44‰ (Pedentchouk *et al.,* 2008; Eley *et al*., 2014). Whilst we potentially see evidence for this seasonality here, with the most isotopically depleted sediment $\delta^2H_{27\text{-}29}$ values occurring during the colder winter months (~-202‰) and the most enriched values occurring in

autumn and spring (~-191‰) (Figure 8), this does not translate into seasonality in apportionment estimates. On reflection, the lack of seasonal apportionment sensitivity most likely reflects the composition of deposited streambed sediments being inherently less dynamic and responsive to catchment processes than fine grained SPM, for example. Streambed sediments represent a cumulative composite of material deposited over a number of days, weeks or months. As such, the delivery of a pulse of δ^2H enriched autumn tree leaf litter to the river, which may be instantly detectable in SPM, would form just the most recent quantitatively insignificant addition to a larger pool of accumulated organic detritus deposited on the streambed. Additionally, autumn leaf litter may remain on the ground for a prolonged period of time before precipitation of sufficient intensity is capable of initiating surface runoff to entrain and transport this organic material to the stream channel.

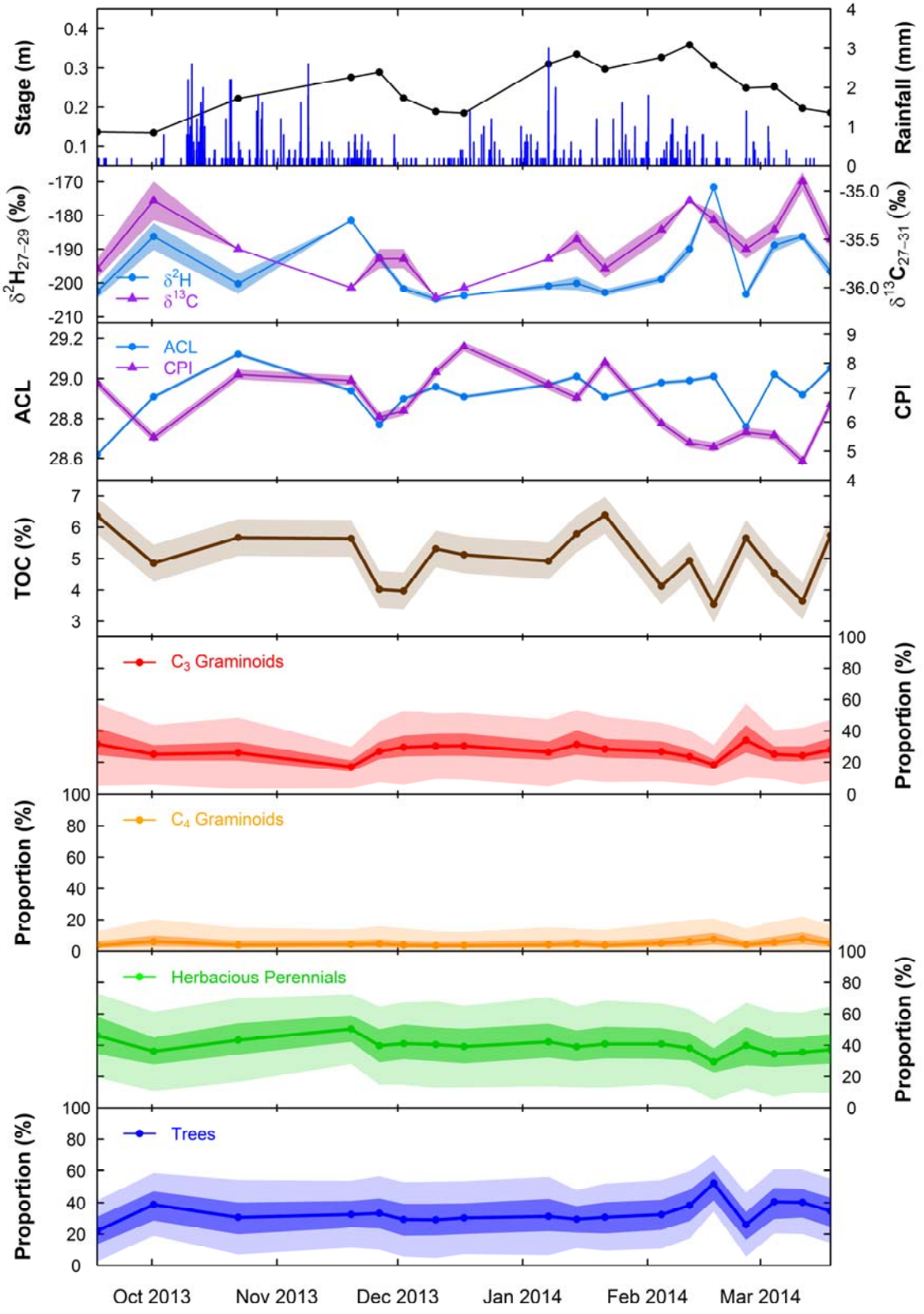

476

477 **Figure 8**: Time-series of organic matter source apportionment estimates and streambed sediment
478 fingerprints for the River Blackwater during September 2013-March 2014. Dark and light shading
479 around median source apportionment estimates represent the 50% and 95% Bayesian credible
480 intervals, respectively. Shading around isotopic ratios and ACL, CPI and TOC measurements
481 represents instrument error.

3.7 Significance and Further Research

The novel data presented here clearly demonstrate that an integrated carbon and hydrogen CSIA of leaf wax *n*-alkanes is an effective approach for quantitatively apportioning plant specific organic matter contributions to streambed sediments within a Bayesian uncertainty framework. In particular, the δ^2H values of leaf waxes proved to be an effective biomarker for differentiating between individual plant species based upon their broad functional type, whilst $\delta^{13}C$ values and *n*-alkane chain length metrics provided complimentary discrimination based on C_3/C_4 physiological differences and different sub-environments, respectively. In contrast to the commonly employed inorganic fingerprints which have been used to discriminate sediment sources based on catchment geology and soil type in previous sediment source apportionment studies (e.g. Martínez-Carreras *et al*. 2010; D'Haen *et al*., 2012), these isotopic differences in *n*-alkane composition offer considerable potential to quantify land-use specific contributions to fluvial organic matter. In this respect, future research could usefully examine if soils under particular plant types are tagged with unique δ^2H and $\delta^{13}C$ signatures, which would allow these isotopes to be used as direct land-use specific soil erosion tracers. There would also be utility in applying these techniques to SPM collected at high-temporal resolution during precipitation events as a means of better understanding organic matter provenance and transport during dynamic high-flow conditions. Finally, examination of a greater variety of cultivated plant species would allow for a more robust assessment of the effectiveness of both $\delta^{13}C$ and δ^2H as discriminators between crop and natural vegetation contributions.

4. CONCLUSIONS

Organic matter is an important constituent of the particulate material transported in fluvial systems, yet techniques capable of quantitatively apportioning its origin have largely been overlooked by the sediment fingerprinting community. Addressing this deficiency, we successfully demonstrate how a novel combined $\delta^{13}C$ and δ^2H compound-specific isotope analysis of *n*-alkane plant lipid extracts can be used as biomarkers to apportion plant specific contributions to fine (<63 μm) streambed sediment organic matter in the lowland, arable, River Blackwater catchment, Norfolk, UK. From the lipid extracts of 18 streambed sediments and 30 individual plant specimens collected from across three sub-environments (aquatic, bankside and terrestrial) and four plant functional types (trees, herbaceous perennials and C_3 and C_4 graminoids), nine isotopic ratio and chain length metrics (ACL, CPI, $\delta^{13}C_{27}$, $\delta^{13}C_{29}$, $\delta^{13}C_{31}$, $\delta^{13}C_{27\text{-}31}$, δ^2H_{27}, δ^2H_{29} and $\delta^2H_{27\text{-}29}$) were derived, which were capable of successfully differentiating 93.1% of plant specimens by functional group. $\delta^2H_{27\text{-}29}$ proved to be the dominant discriminator of plants originating from different functional types, with the largest contrasts arising between trees (-208‰ to -164‰) and C_3 graminoids (259‰ to -221‰). $\delta^{13}C_{27\text{-}31}$ provided effective discrimination between the isotopically enriched C_4 graminoids and the other C_3 plants, whilst also providing discrimination between cultivated and natural vegetation. Neither δ^2H nor $\delta^{13}C$ could

robustly identify plants based on sub-environment, emphasizing a stronger physiological rather than growing environment control over isotopic fractionation. The ACL and CPI were, however, more successful at differentiating plants by sub-environment, indicating such chain length metrics can complement source area identification when used in combination with isotopic ratios. Bayesian mixing model source apportionment results took full account of the uncertainties present whilst revealing considerable temporal variability in plant contributions to streambed sediments during the 7-month period between September 2013 and March 2014. Median contributions ranged from 22-52% for trees, 29-50% for herbaceous perennials, 17-34% for C_3 graminoids and 3-7% from C_4 graminoids, with apportionment exhibiting no apparent seasonality. The results of this study have clearly demonstrated the effectiveness of an integrated carbon and hydrogen CSIA approach for identifying plant specific contributions to streambed sediment organic matter. Future research should further investigate the potential of δ^2H and $\delta^{13}C$ as direct erosion tracers of soils under different land cover types.

ACKNOWLEDGMENTS

RJC acknowledges financial support from a NERC BGS CASE studentship (NE/J500069/1). TK is funded, through IRI THESys, by the German Excellence Initiative. The authors would like to thank Yvette Eley and Rebecca Baldwin for laboratory assistance, Jenny Stevenson, Simon Ellis and Zanist Hama-Aziz for fieldwork support and Gilla Suennenberg for providing the GIS data. This paper is published with the permission of the Executive Director of the British Geological Survey (Natural Environment Research Council).

REFERENCES

Alvarez-Cobelas M, Angeler DG, Sánchez-Carrillo S, Almendros G. 2012. A worldwide view of organic carbon export from catchments. *Biogeochemistry* **107**: 275-293. DOI: 10.1007/s10533-010-9553-z.

Blake WH, Ficken KJ, Taylor P, Russell MA, Walling DE. 2012. Tracing crop-specific sediment sources in agricultural catchments. *Geomorphology* **139-140**: 322-329. DOI:10.1016/j.geomorph.2011.10.036.

Bourbonniere RA, Meyers PA. 1996. Sedimentary geolipid records of historical changes in the watersheds and productivities of lakes Ontario and Erie. *American Society of Limnology and Oceanography* **41**: 352-359.

Broadbent FE. 1953. The soil organic fraction. Advances in Agronomy 5: 153–183.

Bush RT, McInerney FA. 2013. Leaf wax *n*-alkane distributions in and across modern plants: Implications for paleoecology and chemotaxonomy. *Geochimica et Cosmochimica Acta* **117**: 161-179. DOI: 10.1016/j.gca.2013.04.016.

Collins AL, Zhang Y, Walling DE, Grenfell SE, Smith P, Grischeff J, Locke A, Sweetapple A, Brogden D. 2012. Quantifying fine-gained sediment sources in the River Axe catchment, southwest England: application of a Monte Carlo numerical modelling framework

554 incorporating local and genetic algorithm optimization. *Hydrological Processes* **26**: 1962-
555 1983. DOI: 10.1002/hyp.8283.

556 Collins AL, Zhang YS, Duethmann D, Walling DE, Black KS. 2013. Using a novel tracing-tracking
557 framework to source fine-grained sediment loss to watercourses at sub-catchment scale.
558 *Hydrological Processes* **27**: 959-974. DOI: 10.1002/hyp.9652.

559 Cooper RJ, Krueger T, Hiscock KM, Rawlins BG. 2014a. Sensitivity of fluvial sediment source
560 apportionment to mixing model assumptions: A Bayesian model comparison. *Water*
561 *Resources Research* **50**. DOI: 10.1002/2014WR016194.

562 Cooper RJ, Krueger T, Hiscock KM, Rawlins BG. 2014b. High-temporal resolution fluvial sediment
563 source fingerprinting with uncertainty: a Bayesian approach, *Earth Surface Processes and*
564 *Landforms*. DOI: 10.1002/esp.3621.

565 Cooper RJ, Rawlins BG, Lézé B, Krueger T, Hiscock K. 2014c. Combining two filter paper-based
566 analytical methods to monitor temporal variations in the geochemical properties of fluvial
567 suspended particulate matter. *Hydrological Processes* **28**: 4042-4056. DOI: 10.1002/hyp.9945.

568 D'Haen K, Verstraeten G, Dusar B, Degryse P, Haex J, Waelkens M. 2012. Unravelling changing
569 sediment sources in a Mediterranean mountain catchment: a Bayesian fingerprinting approach.
570 *Hydrological Processes* **27**: 896-910. DOI: 10.1002/hyp.9399.

571 Diefendorf AF, Freeman KH, Wing,SL. Graham HV. 2011. Production of *n*-alkyl lipids in living
572 plants and implications for the geologic past. *Geochimica et Cosmochimica Acta* **75**: 7478-
573 7485. DOI: 10.1016/j.gca.2011.09.028.

574 Doucett RR, Marks JC, Blinn DW, Caron M, Hungate BA. 2007. Measuring terrestrial subsides to
575 aquatic food webs using stable isotopes of hydrogen. *Ecology* **88**: 1587-1592. DOI:
576 10.1890/06-1184.

577 Eley Y, Dawson L, Black S, Andrews J, Pedentchouk N. 2014. Understanding $^{2}H/^{1}H$ systematics of
578 leaf wax *n*-alkanes in coastal plants at Stiffkey saltmarsh, Norfolk, UK. *Geochimica et*
579 *Cosmochimica Acta* **128**: 13-28. DOI: 10.1016/j.gca.2013.11.045.

580 Evans DJ, Johnes PJ, Lawrence DS. 2004. Physico-chemical controls on phosphorus cycling in two
581 lowland streams. Part 2 – The sediment phase. *Science of the Total Environment* **329**: 165-182.
582 DOI: 10.1016/j.scitotenv.2004.02.023.

583 Evrard O, Poulenard J, Némery J, Ayrault S, Gratiot N, Duvert C, Prat C, Lefèvre I, Bonté P, Esteves
584 M. 2013. Tracing sediment sources in a tropical highland catchment of central Mexico by
585 using conventional and alterative fingerprinting methods. *Hydrological Processes* **27**: 911-
586 922. DOI: 10.1002/hyp.9421.

587 Farquhar GD, Ehleringer JR, Hubick KT. 1989. Carbon isotope discrimination and photosynthesis.
588 *Annu. Rev. Plant Physiol. Plant Mol. Biol.* **40**: 503-537.

589 Fox JF, Papanicolaou AN. 2007. The use of carbon and nitrogen isotopes to study watershed erosion
590 processes, *Journal of the American Water Resources Association* **43**: 1047-1064. DOI:
591 10.1111/j.1752-1688.2007.00087.x.

592 Hilton J, O'Hare M, Bowes MJ, Jones JI. 2006. How green is my river? A new paradigm of
593 eutrophication in rivers. *Science of the Total Environment* **365:** 66-83.
594 DOI:10.1016/j.scitotenv.2006.02.055.

595 Gibbs MM. 2008. Identifying source soils in contemporary estuarine sediments: A new compound-
596 specific isotope method. *Estuaries and Coasts* **31**: 344-359. DOI 10.1007/s12237-007-9012-9.

597 Guzmán G, Quinton JN, Nearing MA, Mabit L, Gómez JA. 2013. Sediment tracers in water erosion
598 studies: current approaches and challenges. *Journal of Soils and Sediments* **13**, 816-833. DOI:
599 10.1007/s11368-013-0659-5.

600 Hancock GJ, Revill AT. 2013. Erosion source discrimination in a rural Australian catchment using
601 compound-specific isotope analysis (CSIA). *Hydrological Processes* **27**: 923-932. DOI:
602 10.1002/hyp.9466.

603 Horowitz AJ. 2008. Determining annual suspended sediment and sediment-associated trace element
604 and nutrient fluxes. *Science of the Total Environment* **400**: 315-343. DOI:
605 10.1016/j.scitotenv.2008.04.022

606 Hou J, D'Andrea WJ, MacDonald D, Huang Y. 2007. Hydrogen isotopic variability in leaf waxes
607 among terrestrial and aquatic plants around Blood Pond, Massachusetts (USA). *Organic*
608 *Geochemistry* **38**: 977:984. DOI:10.1016/j.orggeochem.2006.12.009.

609 Jeng W-L. 2006. Higher plant *n*-alkane average chain length as an indicator of petrogenic
610 hydrocarbon contamination in marine sediments. *Marine Chemistry* **102**: 242-251. DOI:
611 10.1016/j.marchem.2006.05.001.

612 Koiter AJ, Owens PN, Petticrew EL, Lobb DA. 2013. The behavioral characteristics of sediment
613 properties and their implications for sediment fingerprinting as an approach for identifying
614 sediment sources in river basins. *Earth-Science Reviews* **125**: 24-42. DOI:
615 10.1016/j.earscirev.2013.05.009.

616 Laceby JP, Olley J. 2014. An examination of geochemical modelling approaches to tracing sediment
617 sources incorporating distribution mixing and elemental correlations. *Hydrological Processes*.
618 DOI: 10.1002/hyp.10287.

619 Laceby JP, Olley J, Pietsch TJ, Sheldon F, Bunn SE. 2014. Identifying subsoil sediment sources with
620 carbon and nitrogen stable isotope ratios. *Hydrological Processes*. DOI: 10.1002/hyp.10311.

621 Marshall JD, Brooks JR, Lajtha K. 2007. Sources of variation in the stable isotopic composition of
622 plants. *In* Stable Isotopes in Ecology and Environmental Science (R. Michener and K. Lajtha,
623 Eds.), Blackwell Publishing, pp. 22-60.

624 Martínez-Carreras N, Krein A, Udelhoven T, Gallart F, Iffly JF, Hoffmann L, Pfister L, Walling DE.
625 2010a. A rapid spectral-reflectance-based fingerprinting approach for documenting suspended
626 sediment sources during storm runoff events. *Journal of Soils and Sediments* **10**: 400-413.
627 DOI: 10.1007/s11368-009-0162-1.

628 McConnachie JL, Petticrew EL. 2006. Tracing organic matter sources in riverine suspended
629 sediments: Implications for fine sediment transfers. *Geomorphology* **79**: 13-26.
630 DOI:10.1016/j.geomorph.2005.09.011.

631 McDuffee KE, Eglinton TI, Sessions AL, Sylva S, Wagner T, Hayes JM. 2004. Rapid analysis of ^{13}C
632 in plant-wax *n*-alkanes for reconstruction of terrestrial vegetation signals from aquatic
633 sediments. *Geochemistry, Geophysics, Geosystems* **5** (10) Q10004. DOI:
634 10.1029/2004GC000772.

635 Meyers PA. 1997. Organic geochemical proxies of paleoceanographic, paleolimnologic, and
636 paleoclimatic processes. *Organic Geochemistry* **27**: 213-250.

637 Mukundan R, Walling DE, Gillis AC, Slattery MC, Radcliffe DE. 2012. Sediment source
638 fingerprinting: transforming from a research tool to a management tool. *Journal of the*
639 *American Water Resources Association* **48**: 1241-1257. DOI: 10.1111 / j.1752-
640 1688.2012.00685.x.

641 Némery J, Mano V, Cornella, Etcher H, Mostar F, Me beck M, Belled P, Pore A. 2013. Carbon and
642 suspended sediment transport in an impounded alpine river (Isère, France). *Hydrological*
643 *Processes* **27**: 2498-2508. DOI: 10.1002/hyp.9387.

644 Oeurng C, Savage S, Cornel A, Manuel E, Etcher H, Sánchez-Pérez J-M. 2011. Fluvial transport of
645 suspended sediments and organic matter during flood events in a large agricultural catchment
646 in southwest France. *Hydrological Processes* **25**: 2365-2378. DOI: 10.1002/hyp.7999.

647 O'Leary MH. 1988. Carbon isotopes in photosynthesis. *Bioscience* **38**: 328-336.

648 Pancost RD, Boot CS. 2004. The palaeoclimatic utility of terrestrial biomarkers in marine sediments.
649 *Marine Chemistry* **92**: 239-261. DOI:10.1016/j.marchem.2004.06.029.

650 Parnell AC, Inger R, Bearhop S, Jackson AL. 2010. Source partitioning using stable isotopes: coping
651 with too much variation. *PLoS ONE* **5**: e9672. DOI: 10.1371/journal.pone.0009672.

652 Pedentchouk N, Sumner W, Tipple B, Pagani M. 2008. $\delta^{13}C$ and $\delta^{2}H$ compositions of *n*-alkanes from
653 modern angiosperms and conifers: An experimental set up in central Washing State, USA.
654 *Organic Geochemistry* **39**: 1066-1071. DOI: 10.1016/j.orggeochem.2008.02.005.

655 Plummer M. 2003. JAGS: A program for analysis of Bayesian graphical models using Gibbs
656 sampling. Proceeding of the 3rd international workshop on distributed statistical computing,
657 Vienna, Austria.

658 Pulley S, Foster I, Antunes P. 2015. The uncertainties associated with sediment fingerprinting
659 suspended and recently deposited fluvial sediment in the Nene river basin. *Geomorphology*
660 **228**: 303-319. DOI: 10.1016/j.geomorph.2014.09.016.

661 R Development Core Team. 2014. R: A language and environment for statistical computing. R
662 Foundation for Statistical Computing: Vienna, Austria. http://www.R-project.org.

663 Sachse D, Billault I, Bowen G, Chikaraishi Y, Dawson T, Feakins S, Freeman K, Magill C,
664 McInerney F, van der Meer M, Polissar P, Robins R, Sachs J, Schmidt H, Sessions A, White J,
665 West J, Kahmen A. 2012. Molecular paleohydrology: interpreting the hydrogen-isotopic
666 composition of lipid biomarkers from photosynthesizing organisms. *Annual Review of Earth*
667 *and Planetary Sciences* **40:** 221–249. DOI: 10.1146/annurev-earth-042711-105535.

668 Schindler Wildhaber Y, Liechti R, Alewell C. 2012. Organic matter dynamics and stable isotope
669 signature as tracers of the sources of suspended sediment. *Biogeosciences* **9**: 1985-1996. DOI:
670 1 0.5194/bg-9-1985-2012.

671 Sessions AL, Burgoyne TW, Schimmelmann A, Hayes JM. 1999. Fractionation of hydrogen isotopes
672 in lipid biosynthesis. *Organic Geochemistry* **30**: 1193-1200. DOI: 10.1016/S0146-
673 6380(99)00094-7.

674 Smith HG, Blake WH. 2014. Sediment fingerprinting in agricultural catchments: A critical re-
675 examination of source discrimination and data corrections. *Geomorphology* **204**: 177-191.
676 DOI: 10.1016/j.geomorph.2013.08.00.

677 Thompson J, Cassidy R, Doody DG, Flynn R. 2013. Predicting critical source areas of sediment in
678 headwater catchments. *Agriculture, Ecosystems and Environment* **179**: 41-52. DOI:
679 10.1016/j.agee.2013.07.010.

680 Walling DE. 2005. Tracing suspended sediment sources in catchments and river systems. *Science of*
681 *the Total Environment* **344**: 159-184. DOI: 10.1016/j.scitotenv.2005.02.011.

682 Walling DE. 2013. The evolution of sediment source fingerprinting investigations in fluvial systems.
683 *Journal of Soils and Sediments* **13**: 1658-1675. DOI: 10.1007/s11368-013-0767-2.

684 Wensum Alliance. 2014. River Wensum Demonstration Test Catchment Project. Online:
685 www.wensumalliance.org.uk.

686 Wilkinson SN, Hancock GJ, Bartley R, Hawdon AA, Keen RJ. 2013. Using sediment tracing to assess
687 processes and spatial patterns of erosion in grazed rangelands, Burdekin River basin,
688 Australia. *Agriculture, Ecosystems and Environment* **180**: 90-102. DOI:
689 10.1016/j.agee.2012.02.002.

690 Withers PJA, Jarvie HP. 2008. Delivery and cycling of phosphorous in rivers: A review. *Science of*
691 *the Total Environment* **400**: 379-395. DOI: doi:10.1016/j.scitotenv.2008.08.002.

692 Zech M, Pedentchouk N, Buggle B, Leiber K, Kalbitz K, Marković SB, Glaser B. 2011. Effect of leaf
693 litter degradation and seasonality on D/H isotope ratios of *n*-alkane biomarkers. *Geochimica*
694 *et Cosmochimica Acta* **75**: 4917-4928. DOI: 10.1016/j.gca.2011.06.006.

695 Zhang Z, Zhao M, Eglinton G, Lu H, Huang C-Y. 2006. Leaf wax lipids as paleovegetational and
696 paleoenvironmental proxies for the Chinese Loess Plateau over the last 170 kyr. *Quaternary*
697 *Science Reviews* **25**: 575-594. DOI: 10.1016/j.quascirev.2005.03.009.